

# Reionization of the Intergalactic Medium and its Effect on the CMB

Zoltán Haiman

*NASA/Fermilab Astrophysics Center, Fermi National  
Accelerator Laboratory, Batavia, IL 60510*

Lloyd Knox

*Department of Astronomy and Astrophysics, University of  
Chicago, Chicago, IL 60637*

## Abstract

The bulk of the hydrogen in the universe transformed from neutral to ionized somewhere in the redshift interval  $5 \lesssim z \lesssim 40$ , most likely due to ionizing photons produced by an early generation of stars or mini-quasars. The resulting free electrons, interacting with the CMB photons via Thomson-scattering, are a mixed blessing, providing both a probe of the epoch of the first stars and a contaminant to the pristine primary anisotropy. Here we review our current knowledge of reionization with emphasis on inhomogeneities and describe the possible connections to CMB anisotropy.

*Subject headings:* Reionization, cosmic microwave background, foregrounds

## 1. Introduction

One of the most remarkable observational results in the last three decades in cosmology is the lack of the Gunn–Peterson trough in the spectra of high-redshift quasars and galaxies. This finding implies that the intergalactic medium (IGM) is highly ionized at least out to  $z \sim 5$ , the redshift of the most distant known quasars and galaxies<sup>1</sup>. Since the primeval plasma recombined at  $z \sim 1100$ , its subsequent ionization requires some form of energy injection into the IGM, naturally attributable to astrophysical sources. The two most popular examples of such sources are an early generation of stars, residing in sub-galactic size clusters (hereafter “mini-galaxies”), or accreting massive ( $\sim 10^6 M_\odot$ ) black holes in small ( $\lesssim 10^9 M_\odot$ ) halos (hereafter “mini-quasars”).

Reionization is interesting for a variety of reasons. First, the most fundamental questions are still unanswered: What type of sources caused reionization, and around what redshift did it occur? How were the reionizing sources distributed relative to the gas? What

was the size, geometry, and topology of the ionized zones, and how did these properties evolve? Second, and more directly relevant to the topic of this review, reionization leaves distinctive signatures on the cosmic microwave background (CMB) through the interaction between the CMB photons and free electrons. Although it may complicate the extraction of cosmological parameters from CMB data, this “contamination” could yield important information on the ionization history of the IGM. Through reionization, the CMB is a useful probe of nonlinear processes in the high-redshift universe.

Thomson scattering from free electrons affects the CMB in several ways. Because the scattering leads to a blending of photons from initially different lines of sight, there is a damping of the *primary* temperature anisotropy. On the other hand, a new *secondary* anisotropy is generated by what can be thought of as a Doppler effect: as photons scatter off free electrons, they pick up some of their peculiar momentum. Finally, the polarization dependence of the Thomson cross section creates new polarization from the initially anisotropic photon field.

The inhomogeneity of reionization affects these processes in two different ways. First, the inhomogeneity of the medium affects how the *mean* ionization fraction evolves with time. This is important since the damping, Doppler and polarization effects all occur even in the idealized case of spatially homogeneous reionization. Secondly, the spatial fluctuations in the ionization fraction can greatly enhance the contribution from the Doppler effect at small angular scales. Polarization and damping are much less influenced by the inhomogeneity, as we will see below.

The aim of the present review is to summarize our current knowledge of reionization, describe the possible connections to the CMB, and assess what we can hope to learn about the high-redshift IGM from forthcoming observations of the CMB anisotropies.

## 2. Reionization

### 2.1. Homogeneous Reionization and the Reionization Redshift

If the IGM was neutral, its optical depth to Ly $\alpha$  absorption would be exceedingly high:

$\tau_{\text{igm}} \sim 10^5 (\Omega_b h / 0.03) [(1+z)/6]^{3/2}$ , wiping out the flux from any source at observed wavelengths shorter than  $\lambda_{\text{Ly}\alpha}(1+z)$ . The spectra of high-redshift quasars and galaxies reveal Ly $\alpha$  absorption by numerous discrete Ly $\alpha$  forest clouds, separated in redshift, rather than the continuous Gunn–Peterson (GP) trough expected from a

<sup>1</sup>Currently the best lower limit on the reionization redshift comes from the detection of high- $z$  Ly $\alpha$  emission lines, implying  $z \geq 5.64$  (see discussion below).

neutral IGM. The detection of the continuum flux in-between the Ly $\alpha$  clouds implies that  $\tau_{\text{igm}}$  is at most of order unity, or, equivalently, an upper limit on the average neutral fraction of  $x = n_{\text{HI}}/n_{\text{tot}} \lesssim 10^{-5}$ . The intergalactic medium is therefore highly ionized. Note that there is no sharp physical distinction between the intergalactic medium and the low column density ( $N_{\text{HI}} \lesssim 10^{14} \text{ cm}^{-2}$ ) Ly $\alpha$  forest (Reisenegger & Miralda-Escudé 1995). These Ly $\alpha$  clouds fill most of the volume of the universe, are highly ionized, and account for most of the baryons (implied by Big Bang nucleosynthesis) at high redshift (Weinberg et al. 1997; Rauch et al. 1997).

The energy requirement of reionization can easily be satisfied either by the first mini-galaxies or mini-quasars<sup>2</sup>. Nuclear burning inside stars releases several MeV per hydrogen atom, and thin-disk accretion onto a Schwarzschild black hole releases ten times more energy, while the ionization of a hydrogen atom requires only 13.6 eV. It is therefore sufficient to convert a fraction of  $\lesssim 10^{-5}$  of the baryonic mass into either stars or black holes in order to ionize the rest of the baryons in the universe. In a homogeneous universe, the ratio of recombination time to Hubble time in the IGM is  $t_{\text{rec}}/t_{\text{Hub}} \sim [(1+z)/11]^{-3/2}$  so that each H atom would only recombine a few times at most until the present time. Unless reionization occurred at  $z \gg 10$ , recombinations therefore would not change the above conclusion, and the number of ionizing photons required per atom would be of order unity. Based on three-dimensional simulations, Gnedin & Ostriker (1997) argued that the clumpiness of the gas increases the average global recombination rate by a factor  $C \equiv \langle \rho^2 \rangle / \langle \rho \rangle^2 \sim 30 - 40$  (the averages are taken over the simulation box). This would imply a corresponding increase in the necessary number of ionizing photons per atom. However, in a more detailed picture of reionization in an inhomogeneous universe (Gnedin 1998, Miralda-Escudé et al. 1999), the high-density regions are ionized at a significantly later time than the low density regions. If this picture is correct, then one ionizing photon per atom would suffice to reionize most of the volume (filled by the low-density gas); recombinations from the high-density regions would only contribute to the average recombination rate at a later redshift.

The reionization redshift can be estimated from first principles. In the simplest picture [first discussed by Arons & Wingert (1972) in the context of quasars], a homogeneous neutral IGM is percolated by the individ-

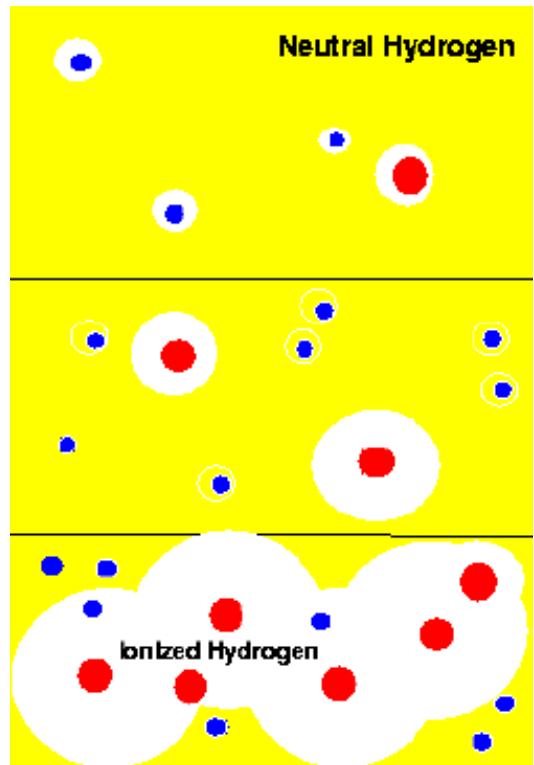


Fig. 1.— Schematic stages of reionization by early mini-galaxies. The small dots denote small halos with  $T_{\text{vir}} < 10^4 \text{ K}$ , the larger dots correspond to larger halos with  $T_{\text{vir}} > 10^4 \text{ K}$ . Top panel –  $z \sim 40$ : The first halos form, both small and large halos create HII zones. Middle panel –  $z \sim 20$ : The UV background suppresses star-formation in small halos, only large halos can produce HII zones. Bottom panel –  $z \sim 15$ : the ionized zones from the large halos overlap.

<sup>2</sup>More exotic possibilities that we do not discuss here include primordial black holes (e.g. Gibilisco 1996); cosmic rays (e.g. Nath & Bierman 1993); winds from supernovae (e.g. Ostriker & Cowie 1981); or decaying neutrinos (Sciama 1993).

ual HII regions growing around each isolated UV source. The universe is reionized when the ionized bubbles overlap, i.e. when the filling factor of HII regions reaches unity<sup>3</sup>. Several authors studied this problem (Carr et al. 1984, Couchman & Rees 1986, Fukugita & Kawasaki 1994, Meiksin & Madau 1993; Shapiro et al. 1994, Tegmark et al. 1994; Aghanim et al. 1996; Haiman & Loeb 1997). Specifically, Haiman & Loeb (1998a) have used the Press–Schechter formalism to describe the formation of halos that potentially host ionizing sources, in order to estimate the redshift at which overlap occurs. In this study, star and quasar black hole formation was allowed only inside halos that can cool efficiently via atomic hydrogen, since molecular hydrogen would be photodissociated earlier, as argued by Haiman, Abel & Rees (1999) and Haiman, Rees & Loeb (1997). This requirement translates to a minimum virial temperature of  $\sim 10^4\text{K}$ , or halo masses above  $\sim 10^8 M_\odot [(1+z)/11]^{-3/2}$  (see Fig. 1). For both types of sources, the total amount of light they produce was calibrated using data from redshifts  $z \lesssim 5$ . The efficiency of early star formation can be estimated from the observed metallicity of the intergalactic medium (Songaila & Cowie 1996, Tytler et al. 1995), utilizing the fact that these metals and the reionizing photons likely originate from the same stellar population. Similarly, the efficiency of black hole formation inside early mini-quasars can be constrained to match the subsequent evolution of the quasar luminosity function at redshifts  $z \lesssim 5$  (Pei 1995). These assumptions generically lead to a reionization redshift  $8 \lesssim z \lesssim 15$ . The uncertainty in the redshift reflects a range of cosmological parameters ( $H_0, \Omega_m, \Omega_b$ ), CDM power spectra ( $n, \sigma_8$ ), and efficiency parameters for the production and escape fraction of ionizing photons. In the stellar reionization scenario, the predicted redshift could be above or below this range, if the initial mass function was strongly biased (relative to Scalo 1986) towards massive or low-mass stars.

## 2.2. Importance and Treatments of Inhomogeneities

Although the naive picture of overlapping HII spheres may give a good estimate for the “overlap redshift”, it is likely to be a crude and incomplete description of the real process of reionization. The ionizing sources are expected to be located in the highly overdense regions that form the complex large scale structure of the universe - along filaments or sheets, or at their intersections (see Fig. 2). The ionizing radiation will have to cross the local dense structures before propagating into

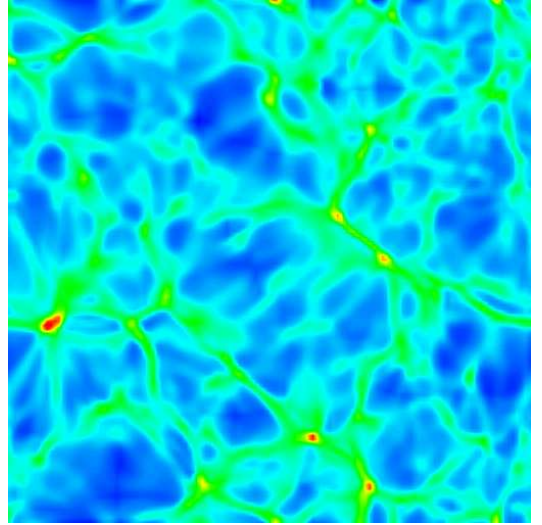


Fig. 2.— A two-dimensional slice of  $\log(\delta_b)$ , the baryonic overdensity at redshift  $z=5$  in a three-dimensional simulation (see Zhang et al. 1998).

the IGM, which itself has significant density fluctuations. Several important consequences of these inhomogeneities can be noted. First, reionization could occur “outside-in” (Miralda-Escudé et al. 1999), if the radiation from a typical source escapes through a relatively narrow solid angle from its host, without causing significant local ionization. In this case, the low-density regions could be ionized significantly earlier than the high-density regions. An important effect in this case could be the shadowing of ionizing radiation by the dense concentrations within the IGM. The same type of shadowing effect was found to be important at low redshift. Based on the number of Ly $\alpha$  absorbers, Madau, Haardt & Rees (1998) have concluded that as much as  $\sim 50\%$  of the UV flux is absorbed by these systems. The redshift at which the IGM becomes optically thin to the ionizing continuum is therefore significantly delayed relative to the overlap epoch, when the ionized zones first percolate. An alternative possibility is that the ionizing sources are densely spaced along filaments, and their radiation ionizes most of the dense filament before escaping into the IGM. In this “inside-out” case, the description of ionized zones surrounding their host source would be more applicable. An important feedback during and after reionization is that the newly established UV background can photo-evaporate the gas from small ( $v_{\text{circ}} \lesssim 10$ ) halos (Shapiro, Raga & Mellema 1997; Barkana & Loeb 1999). A related point, important for the detection of the GP trough, is that at the time of overlap of the HII zones, each individual HII region could still have a non-negligible Ly $\alpha$  optical

<sup>3</sup>The expansion of spherical ionization fronts around steady sources can be calculated analytically (Shapiro & Giroux 1987).

depth, due to its residual HI fraction. The GP trough therefore disappears only from the spectra of individual sources located below the later redshift when the average Ly $\alpha$  optical depth of the IGM drops below unity (Haiman & Loeb 1998b; Miralda-Escudé et al. 1999; Shapiro et al. 1987). Finally, the inhomogeneity of the reionized IGM leads to generation of anisotropies in the CMB which are strongly suppressed in the homogeneous case, as we shall see below.

Reionization is now also being addressed by three-dimensional simulations, which can eventually shed light on some of the above issues. The first such studies approximated radiative transfer by assuming an isotropic radiation field, but were able to take into account the inhomogeneities in the gas distribution (Ostriker & Gnedin 1996; Gnedin & Ostriker 1997). The resulting reionization redshift of  $z \sim 7$  in a  $\Lambda$ CDM model is in good agreement with the semi-analytical estimates, given the differences in the assumed cosmology, power spectra, and star formation efficiency. However, an isotropic radiation field is necessarily a crude approximation, at least in the beginning stages of reionization, when each source still has its own isolated ionized zone. In order to understand the progressive overlap of ionized zones, including effects such as self-shielding and shadowing by dense clumps, it is necessary to incorporate radiative transfer into three dimensional simulations (Norman et al. 1998). The numerical algorithms for the first such attempts are described in Abel, Norman & Madau (1998) and Razoumov & Scott (1998). Results from an approximate treatment (Gnedin 1998) also support the outside-in picture of reionization described above.

### 2.3. The Nature of Reionizing Sources

Several authors have emphasized that the known population of quasars or galaxies provide  $\sim 10$  times fewer ionizing photons than necessary to reionize the universe (see, e.g. Shapiro et al. 1994, or Madau et al. 1999, and references therein). The two most natural candidates for undetected ionizing sources are the mini-galaxies and mini-quasars expected to be associated with small ( $\sim 10^{8-10} M_\odot$ ) dark halos at  $z \sim 10$ . As there are no compelling *ab initio* theoretical arguments to strongly favor one type of source over the other, the best hope is to distinguish these two possibilities from observations. One expects at least three major differences between mini-galaxies and mini-quasars: their spectra, their absolute brightness (or, alternatively, space density), and the angular size of their luminous regions.

The flux from stellar populations drops rapidly with frequency above the ionization threshold of hydrogen, while the spectra of mini-quasars are expected to be

harder and extend into the X-ray regime. Stars could therefore not reionize HeII, while quasars with typical spectra (Elvis et al. 1994) would reionize HeII at approximately the same redshift as H (Haiman & Loeb 1998a). However, recent high-resolution spectra of  $z \sim 3$  quasars have shown a widely fluctuating HeII/HI optical depth (Reimers et al. 1997). The authors interpreted this observation as evidence for HeIII regions embedded in an otherwise HeII medium, i.e. a detection of the HeII reionization epoch (see also Wadsley et al. 1998). If this interpretation is verified by future data, it would constrain the number of mini-quasars with hard spectra extending to X-rays at high redshifts (Haiman & Loeb 1998b; Miralda-Escudé 1998; Miralda-Escudé & Rees 1994). At present, a plausible alternative interpretation of the HeII observations is that the observed HeII optical depth fluctuations are caused by statistical fluctuations in the IGM density or the ionizing background flux (Miralda-Escudé et al. 1999), rather than by the patchy structure of HeII/HeIII zones.

The X-ray background (XRB; Miyaji et al. 1998; Fabian & Barcons 1992) might provide another useful constraint on mini-quasar models with hard spectra (Haiman & Loeb 1998c). These models overpredict the *unresolved flux* by a factor of  $\sim 2 - 7$  in the 0.1–1 keV range. If an even larger fraction of the XRB will be resolved into low-redshift AGNs in the future, then the XRB could be used to place more stringent constraints on the X-ray spectrum or the abundance of the mini-quasars.

A second distinction between galaxies and quasars can be made based on their absolute luminosity and space density. On average, based on their  $z < 5$  counterparts, high-redshift mini-quasars are expected to be roughly  $\sim 100$  times brighter, but  $\sim 100$  times more rare, than galaxies. At the overlap epoch, HII regions from mini-quasars would therefore be larger but fewer than those from mini-galaxies. The typical size and abundance of HII regions has at least three important implications. First, it affects the CMB anisotropies; the larger the HII regions, the larger the effect on the CMB (Gruzinov and Hu 1998, Knox et al. 1998), as we will see below. Second, large enough HII regions ( $\gtrsim 1$  Mpc) would allow gaps to open up in the GP trough; the flux transmitted through such gaps around very bright quasars could be detectable (Miralda-Escudé et al. 1999). Third, if sources form inside the rare, high- $\sigma$  peaks, they would be strongly clustered (Knox et al. 1998). This clustering would increase the effective luminosity of each source, and would enhance both of the effects above.

Finally, a constraint on the number of mini-quasars at  $z > 3.5$  can be derived from the Hubble Deep Field

(HDF). Mini-quasars are expected to appear as faint point-sources in the HDF, unless their underlying extended host galaxies are resolved. The properties of faint *extended* sources found in the Hubble Deep Field (HDF) agree with detailed semi-analytic models of galaxy formation (Baugh et al. 1998). On the other hand, the HDF has revealed only a handful of faint *unresolved* sources, and none with the colors expected for high redshift quasars (Conti et al. 1999). The simplest mini-quasar models predict the existence of  $\sim 10 - 15$  B-band “dropouts” in the HDF, inconsistent with the lack of detection of such dropouts up to the  $\sim 50\%$  completeness limit at  $V \approx 29$ . To reconcile the models with the data, a mechanism is needed that suppresses the formation of quasars in halos with circular velocities  $v_{\text{circ}} \lesssim 50 - 75 \text{ km s}^{-1}$  (Haiman, Madau & Loeb 1999). This suppression naturally arises due to the photo-ionization heating of the intergalactic gas by the UV background after reionization. Forthcoming data on point-sources from NICMOS observations of the HDF (see Thompson et al. 1998) could further improve these constraints.

#### 2.4. When was the Universe Reionized?

As described above, theoretical expectations place the reionization redshift at  $8 \lesssim z \lesssim 15$ . What about observations? At present, the best *lower* limit in the reionization redshift comes from the detection of high-redshift Ly $\alpha$  emitters (Hu et al. 1998; Weymann et al. 1998). As argued by Miralda-Escudé (1998), the damping wing of Ly $\alpha$  absorption by a neutral IGM has a large residual optical depth that would severely damp any Ly $\alpha$  emission line. Currently the highest redshift at which a Ly $\alpha$  emitter is seen is  $z = 5.64$ ; the existence of this object implies that reionization occurred prior to this redshift (see Haiman & Spaans 1998). Note that HII regions around individual sources, excepting only the brightest quasars, would be too small to allow the escape of Ly $\alpha$  photons, because the damping wings of the GP troughs around the HII region would still overlap.

The best *upper* limit on the reionization redshift can be obtained from the CMB anisotropy data. Several experiments have revealed a rise in the power on small angular scales, and a drop at even smaller scales (e.g., Bond et al. 1999), showing evidence for the first Doppler peak expected from acoustic oscillations in the baryon-photon fluid prior to recombination (e.g., Hu & Sugiyama 1994). These observations can also be used to set limits on the electron scattering optical depth (or the corresponding reionization redshift) that would suppress the Doppler peak. From a compilation of all the existing measurements, Griffiths et al. (1998) have derived the stringent

(although model-dependent) constraint  $z \lesssim 40$  on the reionization redshift – if reionization occurred earlier, the electron scattering optical depth would have reduced the amplitude of the anisotropies below the observed level. Note that another upper limit results from the spectral distortion of the CMB caused by scattering on the reionized IGM, which is constrained by the upper limit on the Compton  $y$ -parameter measured by COBE. The inferred upper limit on the reionization redshift, however, is much weaker,  $z \lesssim 400$  for typical parameters in a low-density universe (Griffiths et al. 1998, see also Stebbins & Silk 1986). In summary, present observations have narrowed down the possible redshift of the reionization epoch to  $6 \lesssim z \lesssim 40$ , a relatively narrow range that is in good agreement with the theoretical predictions described above.

#### 2.5. Future Observational Signatures

Further observational progress in probing the reionization epoch could come either from the *Next Generation Space Telescope* (NGST), or from more precise measurements of the CMB anisotropies by MAP<sup>4</sup> and Planck<sup>5</sup>. NGST, scheduled for launch in 2007, is expected to reach the  $\sim 1 \text{ nJy}$  sensitivity<sup>6</sup> required to detect individual sources to  $z \sim 10$ , and to perform medium-resolution spectroscopy to  $z \sim 8$ . If reionization occurred close to the low end of the allowed redshift range,  $6 \lesssim z \lesssim 8$ , then it may be possible to infer the redshift directly from the spectra of bright sources. One specific method relies on the spectrum of a bright source just beyond the reionization redshift, so that the individual Ly $\alpha$ , Ly $\beta$ , and other GP troughs do not overlap in frequency, leaving gaps of transmitted flux (Haiman & Loeb 1998b). The measurement of this transmitted flux would be possible with NGST, despite absorption by the high-redshift Ly $\alpha$  forest, as long as the number density of absorbers does not rise much more steeply with redshift than an extrapolation of the current  $z < 5$  data would imply (Fardal et al. 1998). If reionization is gradual, rather than abrupt, than this method would measure the redshift at which the GP optical depth drops to near unity, i.e. the final stages of the reionization epoch. An alternative signature to look for would be the precise shape of the damping wing of Ly $\alpha$  absorption from the neutral IGM along the line of sight to the source (Miralda-Escudé 1998). The shape, if measured by high-resolution spectroscopy, could be used to determine the total optical depth of the

<sup>4</sup><http://map.gsfc.nasa.gov>

<sup>5</sup><http://astro.estec.esa.nl/SA-general/Projects/Planck>

<sup>6</sup>See the NGST Exposure Time Calculator at <http://augusta.stsci.edu>.

IGM. The caveat of this method is the inability to distinguish the neutral IGM from a damped Ly $\alpha$  absorber along the line of sight, close to the source.

An alternative signature is the background Ly $\alpha$  emission from the reionization epoch. Recombinations are slow both at high redshifts, when the IGM is still neutral, and at low redshifts when the IGM density is low. As shown by simulations (Gnedin & Ostriker 1997), the global recombination rate has a pronounced peak around the reionization epoch. The resulting recombinant Ly $\alpha$  emission has been computed by Baltz, Gnedin & Silk (1998), and a detailed detectability study has shown that this signal could be measured by *NGST*, or perhaps even by *HST* (Shaver et al. 1999).

Yet another signature could result from the 21 cm hyperfine transitions in the IGM before reionization. Prior to reionization, the excitation of the 21 cm line in neutral HI atoms depends on the spin temperature. The coupling of the spin temperature to that of the CMB is determined by the local gas density, temperature, and the radiation background from the first mini-galaxies and mini-quasars. In general, the 21 cm line could be seen either in absorption or emission against the CMB, and could serve as a 'tomographic' tool to diagnose the density and temperature of the high redshift neutral gas (see, e.g. Madau et al. 1997; Scott & Rees 1990). If reionization occurred at  $6 \lesssim z \lesssim 10$ , the redshifted 21 cm signals would be detectable by the Giant Metrewave Radio Telescope; a study of the effect at higher redshifts would be possible with next generation instruments such as the THousand Element Array, or the Square Kilometer Array (Shaver et al. 1999).

The reionization redshift could turn out to be closer to the high end of the allowed range,  $10 \lesssim z \lesssim 40$ , rendering direct detection of emission from the reionization epoch implausible (except perhaps the 21cm signal). There is, however, a fortunate "complementarity", since the electron scattering optical depth increases with reionization redshift. Due to the effect on the polarization power spectrum on large angular scales, *MAP* and *Planck* may be able to discern an electron scattering optical depth as small as a few percent (Zaldarriaga et al. 1997, Eisenstein et al. 1998, Prunet et al. 1998). By temperature anisotropy data alone, they may be able to determine an optical depth as small as  $\sim 20\%$  due to the damping effect mentioned earlier—and to be discussed in more detail later.

The reionizing sources may also change the spectral shape of the CMB. The dust that is inevitably produced by the first type II supernovae, absorbs the UV emission from early stars and mini-quasars and re-emits this energy at longer wavelengths. Loeb & Haiman

(1997) have quantified the resulting spectral distortion in Press–Schechter type models, assuming that each type II supernova in a Scalo IMF yields  $0.3M_{\odot}$  of dust with the wavelength-dependent opacity of Galactic dust, uniformly distributed throughout the intergalactic medium. Under these assumptions, the dust remains cold (close to the CMB temperature), and its emission peaks near the CMB peak. The resulting spectral distortion can be expressed as a Compton  $y$ -parameter  $\sim 10^{-5}$ , near the upper limit derived from measurement of the CMB spectrum by COBE (Fixsen et al. 1996). A substantial fraction ( $\sim 10$ –50%) of this total  $y$ -parameter results simply from the direct far-infrared emission by early mini-quasars and could be present even in the absence of any intergalactic dust.

Inhomogeneities in the dust distribution could change these conclusions. Instead of being homogeneously mixed into the IGM, the high-redshift dust may remain concentrated inside or around the galaxies where it is produced. In this case, the average dust particle would see a higher flux than assumed in Loeb & Haiman (1997), so that the dust temperature would be higher, and dust emission would peak at a shorter wavelength. The magnitude of the spectral distortion would be enhanced, and may account for the recently discovered cosmic infrared background (Puget et al. 1996, Schlegel et al. 1998, Fixsen et al. 1998, Hauser et al. 1998) as shown by the semi-analytic models of Baugh et al. (1998). An angular fluctuation in the magnitude of the distortion would also be expected in this case, reflecting the discrete nature of the sources contributing to the effect.

As seen above, reionization has several consequences; in the rest of this review we focus on the connection to the CMB, and the effects of inhomogeneities.

### 3. Effect on the CMB

In this section, we give an in-depth treatment of the effects on the CMB photons of Thomson-scattering off of the free electrons produced by reionization. After defining the optical depth and giving its dependence on the redshift of reionization and cosmological parameters, we discuss the three separate effects: damping, Doppler and polarization generation. Then we derive the evolution equations from the Boltzmann equation, argue that the Doppler effect is the most important *inhomogeneous* effect, and calculate the resulting power spectrum for several simple models of inhomogeneous reionization (IHR).

The probability of a photon scattering in the time interval from some initial time  $t_i$  to the present,  $t_0$  is given

by  $1 - e^{-\tau(t_0)}$  where

$$\tau(t_0) \equiv \int_{t_i}^{t_0} \sigma_T n_e(t) dt \quad (1)$$

is the optical depth to Thomson scattering and  $\sigma_T$  is the Thomson cross-section. If one assumes a step-function transition from a neutral to an ionized IGM at a redshift of  $z_{\text{ion}}$ , the mean optical depth is given by (e.g., Griffiths et al., 1998)

$$\tau(z_{\text{ion}}) = \tau^* / \Omega_0 \left[ \left( 1 - \Omega_0 + \Omega_0 (1 + z_{\text{ion}})^3 \right)^{1/2} - 1 \right] \quad (2)$$

where

$$\tau^* = \frac{H_0 \Omega_b \sigma_T}{4\pi G m_p} \times (1 - Y/2) \simeq 0.033 \Omega_b h, \quad (3)$$

$\Omega_b$  and  $\Omega_0$  are the density of baryonic matter and of all matter respectively, in units of the critical density today,  $H_0$  is the Hubble constant,  $H_0 = 100h \text{ km sec}^{-1} \text{ Mpc}^{-1}$ ,  $G$  is Newton's constant,  $m_p$  is the proton mass and  $Y$  is the mass fraction of baryons in helium. The final equality assumes  $Y = 0.24$ . To get equation 2, we assumed that  $n_e \propto (1+z)^3$ , and adopted the line element,  $dz/dt$ , of a spatially flat universe with only non-relativistic matter and a cosmological constant.

Note that for  $z_{\text{ion}} = 5.64$  (the observational lower bound),  $\Omega_b h^2 = 0.02$  and  $h = 0.65$ , we get  $\tau = 0.016$  for  $\Omega_0 = 1$  and  $\tau = 0.049$  for  $\Omega_0 = 0.3$ . For  $z_{\text{ion}}$  only slightly larger than this limiting value, it is a good approximation to rewrite equation 2 as

$$\tau(z_{\text{ion}}) = 0.037 / \sqrt{\Omega_0} \left( \frac{1 + z_{\text{ion}}}{11} \right)^{3/2} \left( \frac{\Omega_b h^2}{0.02} \right) \left( \frac{0.65}{h} \right). \quad (4)$$

Thus we see that the fraction of CMB photons that have been scattered may be very small, but that this fraction grows fairly rapidly with increasing redshift. The increase in optical depth for fixed  $z_{\text{ion}}$  with increasing  $1 - \Omega_0$  is due to the fact that the proper time from the present to  $z_{\text{ion}}$  increases as the cosmological constant increases.

### 3.1. Simple Arguments

Here we give simple arguments about the nature of the damping, Doppler and polarization effects. Before doing so, it is useful to define the two-point correlation function,  $C(\theta)$  which is perhaps the most important statistical property of the CMB fluctuations:

$$C(\theta) \equiv \langle \Delta(\hat{\gamma}_1, \mathbf{x}, \eta_0) \Delta(\hat{\gamma}_2, \mathbf{x}, \eta_0) \rangle; \cos \theta \equiv \hat{\gamma}_1 \cdot \hat{\gamma}_2 \quad (5)$$

where  $\langle \dots \rangle$  denotes ensemble average. The same information is contained in its Legendre transform, the angular power spectrum,  $C_\ell$ :

$$C(\theta) = \sum_{\ell} \frac{2\ell + 1}{4\pi} C_\ell P_\ell(\cos \theta). \quad (6)$$

Roughly speaking,  $C_\ell$  is the power in modes with wavelength  $\pi/\ell$  so that  $\ell = 180$  corresponds to about a degree. If the fluctuations are Gaussian-distributed and statistically isotropic, all other statistics can be derived from  $C_\ell$ .

#### 3.1.1. Damping

For an initially homogeneous and isotropic photon field, there is just as much probability to scatter into a line of sight as there is to scatter out of it. Therefore, the optical depth to scattering produces no net effect. If, however, there is initial anisotropy, then this anisotropy is damped. Consider a line of sight along which the temperature differs by  $\Delta T$  from the mean  $\bar{T}$  in the absence of damping. If damping is present, then the temperature is changed to

$$\begin{aligned} \bar{T} + \Delta T &\rightarrow (\bar{T} + \Delta T) - (\bar{T} + \Delta T) (1 - e^{-\tau}) + \bar{T} (1 - e^{-\tau}) \\ &\rightarrow \bar{T} + \Delta T e^{-\tau} \end{aligned} \quad (7)$$

This equation expresses the fact that the final temperature is given by the initial temperature, reduced by the photons that have been lost, and increased by the photons that have been scattered in from other lines of sight. Since the photons that have been scattered in come from many different lines of sight, their average temperature is very nearly the global average—an assumption made in equation 7. The net result is that  $\Delta T \rightarrow \Delta T e^{-\tau}$  and therefore  $C(\theta) \rightarrow C(\theta) e^{-2\tau}$  or  $C_\ell \rightarrow C_\ell e^{-2\tau}$ . This simple calculation would imply that the damping is independent of scale, which is not exactly true. Our assumption that the average  $T$  along lines of sight that scattered in equals the global average holds only when the distance *between* the scattering surfaces is much larger than the length scale of interest. At very large angular scales, the damping does not occur, as one would expect from simple causality considerations.

More precisely, the damping factor is  $l$ -dependent and, defined via  $C_\ell = R_\ell^2 C_\ell^{\text{primary}}$ , is given by the fitting formula of Hu & White 1997:

$$R_\ell^2 = \frac{1 - \exp(-2\tau)}{a + c_1 x + c_2 x^2 + c_3 x^3 + c_4 x^4} + \exp(-2\tau), \quad (8)$$

with  $x = l/(l_r + 1)$  and  $c_1 = -0.267, c_2 = 0.581, c_3 = -0.172$  and  $c_4 = -0.0312$ . The characteristic angular



scale  $l_r$  is roughly the angular scale subtended by the horizon at the new last-scattering surface and is given approximately by (Griffiths et al. 1998, Hu & White 1997):

$$l_r = (1 + z_{\text{ion}})^{1/2} (1 + 0.84 \ln \Omega_0) - 1. \quad (9)$$

If not for the  $l$ -dependence, the damping effect would be completely degenerate with the amplitude of the primary power spectrum; i.e., their effects would be indistinguishable. The similar response to amplitude and  $\tau$  over a large range of  $l$  makes them approximately degenerate and is the reason why the optical depth can only be determined to about 10% (Zaldarriaga et al. 1997) or possibly worse (Eisenstein et al. 1998) based on temperature anisotropy alone.

### 3.1.2. Polarization

The Thomson scattering *differential* cross-section is polarization-dependent, and therefore the scattered radiation may be polarized even if the incident radiation is not. However, by symmetry considerations alone one can see that initially isotropic radiation will not become polarized<sup>7</sup>. In fact, it is easy to show that the particular anisotropy required for the creation of polarization is a quadrupole moment. This is essentially due to the  $\cos 2\theta$  dependence of the differential cross-section.

The Fourier analogue of the angle-distance relation can be written as  $\ell \sim (\eta - \eta_*)k$  where  $k$  is the comoving wave-number that projects from conformal time  $\eta_*$  into multipole moment  $\ell$  at conformal time  $\eta$ . Conformal time is related to proper time by  $d\eta = dt/a$  where  $a$  is the scale factor of the expansion. Applying this relationship twice, and using the fact that polarization is generated by the quadrupole moment,  $\ell = 2$ , we find

$$\ell_p \sim (\eta_0 - \eta_{\text{ion}}) \left( \frac{2}{\eta_{\text{ion}} - \eta_{\text{LSS}}} \right) \simeq 2 (\sqrt{z_{\text{ion}} + 1} - 1). \quad (10)$$

For the last equality, we assumed a matter-dominated Universe and that  $\eta_{\text{ion}} \gg \eta_{\text{LSS}}$ . Thus we expect a peak in the polarization power spectrum near  $\ell_p \sim 2z_{\text{ion}}^{1/2}$ .

Determining the location of this peak allows one to determine the epoch of reionization. The amplitude of the peak is proportional to the optical depth, and thus also helps in determining  $z_{\text{ion}}$ . Unfortunately, the signal is very weak and present only at large angular scales, e.g.,  $\ell_p \simeq 5$  for  $z_{\text{ion}} = 10$ . Since there are only  $2l + 1$  independent modes from which to determine  $C_l$ , sample variance is worst at low  $l$ . Also, the large-scale features of

polarization maps reconstructed from time-ordered data are likely to be those most sensitive to systematic errors. Finally, polarized galactic foregrounds (dust and synchrotron) are expected to be most troublesome at small  $l$  (Bouchet et al. 1998, Knox 1998). However, a benefit of the low- $\ell$  location of this signature is that if it can be measured, its interpretation will not be complicated by the inhomogeneity of the reionization, which is a much smaller-scale phenomenon.

If the systematic errors are negligible, the reionization feature in the polarization power spectrum can be used to discern very small optical depths. Forecasts of parameter determination by Eisenstein et al. (1998) using both the temperature anisotropy and polarization data are for one sigma errors on  $\tau$  of 0.022 for *MAP* and 0.004 for *Planck*. Also see Zaldarriaga et al. (1997) for similar results. Note that these sensitivities, especially in the case of *Planck*, are high enough to detect the effects of reionization *at any epoch* given that we know it happened prior to  $z = 5.64$ .

### 3.1.3. Doppler Effect

The contribution to  $\Delta T/T$  at location  $\mathbf{x}_0$ , in direction  $\hat{\gamma}$ , at conformal time  $\eta_0$  (today) is given by

$$\frac{\Delta T}{T}(\mathbf{x}_0, \hat{\gamma}, \eta_0) = \sigma_T \int_{\eta_{\text{ion}}}^{\eta_0} d\eta n_e(\mathbf{x}) \hat{\gamma} \cdot \mathbf{v}_e(\mathbf{x}) a \quad (11)$$

where  $\mathbf{x} = \mathbf{x}_0 + \hat{\gamma}(\eta_0 - \eta)$ . As one might expect, it is proportional to the line-of-sight integral of the parallel component of electron velocity,  $\mathbf{v}_e$  times the number density of scatterers,  $n_e$ .

As Sunyaev (1978) and Kaiser (1984) pointed out, in the homogeneous case this contribution to  $\frac{\Delta T}{T}$  is suppressed by cancellations due to oscillations in  $\mathbf{v}_e$ . One way to think of these cancellations is that photons get nearly opposite Doppler shifts on different sides of a density peak, which is a consequence of potential flows generated by gravitational instability. The cancellations are less complete at large angular scales ( $l \lesssim 100$ ) and there is a measurable effect which is exactly taken into account in Boltzmann codes such as CMBFAST<sup>8</sup>. If speed is critical, the fitting formulae of Griffiths et al. (1998) can be employed for an approximate treatment.

The cancellations at small scales can be greatly reduced by the modulation of the number density of free electrons which we can write as  $n_e = x_e n_p$  where  $x_e$  is the ionization fraction and  $n_p$  is the number density of all protons, including those in H and He. This modulation occurs even in the case of homogeneous reionization

<sup>7</sup>Unless the electron spins are aligned, perhaps by a magnetic field.

<sup>8</sup> <http://www.sns.ias.edu/~matiasz/CMBFAST/cmbfast.html>



(spatially constant  $x_e$ ) due to spatial variations in  $n_p$ . Because  $v_e$  is zero to zeroth order, and  $n_p$  is uniform to zeroth order, this is a second-order effect. That this second order effect could dominate the first-order one (which is small due to cancellations) was pointed out by Ostriker and Vishniac and is known as the Ostriker-Vishniac effect (Ostriker & Vishniac 1986, Vishniac 1987). Subsequent systematic study of all 2nd order contributions have shown that it is the dominant second-order contribution as well (Hu et al. 1994, Dodelson & Jubas 1995).

Another source of modulation of the number density of free electrons is spatial variations in  $x_e$ , i.e., IHR. As a photon streams towards us from the last-scattering surface, it may pick up a Doppler “up kick” on one side of an overdensity, but avoid the canceling “down kick” on the other because the IGM there is still neutral. How effectively the cancellation is avoided depends on the matching between the typical sizes of the ionized domains and the correlation length of the velocity field, as we will discuss below.

### 3.2. Evolution Equations

We now derive equation 11, as well as a more general expression which includes the contribution from damping as well. More complete treatments of the evolution of a photon distribution function in an expanding, inhomogeneous Universe can be found in, e.g., Ma & Bertschinger (1995).

The Boltzmann equation governing the evolution of the photon phase-space distribution function,  $f$ , is simply  $\frac{df}{dt} = C$ , where  $C$  takes into account the effect of collisions—in this case with electrons via Thomson scattering. The Thomson scattering cross-section is independent of frequency and therefore does not induce spectral distortions; the effect on the distribution function can be fully described by the change in brightness. Thus we use the brightness perturbation variable defined by  $\Delta \equiv (\partial f_0 / \partial q)^{-1} f_1$  where  $q$  is the comoving photon momentum, and the phase-space distribution function has been partitioned into a homogeneous and inhomogeneous part,  $f = f_0 + f_1$ . For a Planckian  $f$  with thermal fluctuations,  $\Delta T$ , about a mean temperature of  $T$ ,  $\Delta = 4\Delta T/T$ .

Expanding the total derivative on  $f$ , keeping terms to first order in the perturbation variables and Fourier transforming the result, the Boltzmann equation becomes:

$$\begin{aligned} \dot{\tilde{\Delta}}(\mathbf{k}, \hat{\gamma}, \eta) + ik\mu \tilde{\Delta}(\mathbf{k}, \hat{\gamma}, \eta) + \frac{2}{3} \dot{h}(\mathbf{k}, \eta) \\ + \frac{2}{3} \left( 3\dot{h}_{33}(\mathbf{k}, \eta) - \dot{h}(\mathbf{k}, \eta) \right) P_2(\mu) = \end{aligned}$$

$$\int d^3x e^{i\mathbf{k} \cdot \mathbf{x}} \dot{\tau}(\mathbf{x}, \eta) S(\mathbf{x}, \hat{\gamma}, \eta) \quad (12)$$

where  $\tilde{\Delta}$  is the Fourier transform of the brightness perturbation,  $\hat{\gamma}$  is the direction of the photon momentum,  $\mu \equiv \hat{k} \cdot \hat{\gamma}$ , the dot indicates differentiation with respect to conformal time and  $h_{33}$  and  $h$  are the 3,3 component and trace of the synchronous gauge metric perturbation, respectively, in the coordinate system defined by  $x_3 = \hat{\gamma}$ .

On the right-hand side of equation (12) we have explicitly separated out the dependence of the collision term on the differential optical depth,  $\dot{\tau} = a\sigma_T n_e(\mathbf{x}, \eta)$ . The quantity  $S$  is a function of the brightness perturbation and the electron velocity. To first order in the perturbation variables its Fourier transform is (neglecting the polarization dependence of the Thomson cross-section)

$$\tilde{S}(\mathbf{k}, \hat{\gamma}, \eta) = -\tilde{\Delta} + \tilde{\Delta}_0 + 4\hat{\gamma} \cdot \mathbf{v}_e - \frac{1}{2} \tilde{\Delta}_2 P_2(\mu) \quad (13)$$

where  $\Delta = \sum_{\ell} (2\ell + 1) \Delta_{\ell} P_{\ell}(\mu)$ .

If we were to allow both  $\dot{\tau}$  and  $S$  to depend on  $\mathbf{x}$ , the Fourier modes would no longer evolve independently. To avoid this complication, we use an expansion in small  $\dot{\tau}$ . Let  $\tilde{\Delta}^{(0)}$  be the solution for  $\dot{\tau} \equiv 0$  and let  $\tilde{\Delta}^{(1)} = \tilde{\Delta} - \tilde{\Delta}^{(0)}$ . Then to first order in  $\dot{\tau}$ :

$$\dot{\tilde{\Delta}}^{(1)}(\mathbf{k}) + ik\mu \tilde{\Delta}^{(1)}(\mathbf{k}) = \int d^3x e^{i\mathbf{k} \cdot \mathbf{x}} \dot{\tau}(\mathbf{x}) S^{(0)}(\mathbf{x}, \hat{\gamma}). \quad (14)$$

which has the solution in real space:

$$\Delta^{(1)}(\hat{\gamma}, \mathbf{x}, \eta_0) = \int_{\eta_i}^{\eta_0} d\eta' \dot{\tau}(\mathbf{x}') S^{(0)}(\mathbf{x}', \hat{\gamma}) \quad (15)$$

where  $\mathbf{x}' = \mathbf{x} + \hat{\gamma}(\eta_0 - \eta')$ . This solution can be derived with a Green function approach or simply verified by substitution. It can be taken to higher order, if desired, by getting  $\Delta^{(2)}$  from  $S^{(1)}$ , etc. Note that for the Doppler effect equation 15 is exact because  $v_e$  (unlike, e.g.,  $\Delta$ ) receives no corrections due to the optical depth.

We can now argue that the Doppler effect, due to the  $\mathbf{v}_e$  term in equation 15, is the most important inhomogeneous effect. The dominance of this effect is due to the fact that by the time of reionization, velocities have grown substantially as they react to the gravitational field. On the relevant length scales, the rms peculiar velocities are about  $10^{-3}$ . In contrast, the damping of the anisotropy is due to the  $-\Delta$  term in  $S$ , which has not grown from its primordial value of  $10^{-5}$ . Similarly, polarization is sourced by the quadrupole moment which is also still at the  $10^{-5}$  level at the epoch of reionization. Therefore we expect these contributions to be down by two orders of magnitude in amplitude, or four in power.

If we break up the correlation function into components according to the expansion in optical depth:

$$C(\theta) = C^{(0)}(\theta) + 2C^{(01)}(\theta) + C^{(1)}(\theta) \quad (16)$$

where  $C^{(0)}$ ,  $C^{(1)}$  and  $C^{(01)}$  are the correlations between the two zeroth order terms, between the two first order corrections and between the first order and zeroth order terms, respectively.

For the Doppler effect, the (exact) correction to the homogeneous case comes entirely from the  $C^{(1)}$  term which is equal to

$$C^{(1)}(\theta) = \int_{\eta_i}^{\eta_0} d\eta_1 \int_{\eta_i}^{\eta_0} d\eta_2 \langle (\hat{\tau}\hat{\gamma}_1 \cdot \mathbf{v}_e)_1 (\hat{\tau}\hat{\gamma}_2 \cdot \mathbf{v}_e)_2 \rangle \quad (17)$$

where the numeric subscript on the quantities in parentheses means evaluate at, e.g.,  $(\mathbf{x} + \hat{\gamma}_1(\eta_0 - \eta_1), \eta_1)$ .

From equation 17 we see that the relevant quantity for the CMB 2-point autocorrelation function, is the two-point function of the product,  $\hat{\tau}\hat{\gamma} \cdot \mathbf{v}_e$ , integrated over the lines of sight. As pointed out by Knox et al. (1998) it is this latter 2-point function which must be calculated from either simulations or analytical models of the reionization process.

### 3.3. Results from Simple Models

A very simple toy model was used by Gruzinov and Hu (1998, hereafter GH) and by Knox et al. (1998, hereafter KSD) for investigating the effect of IHR on the power spectrum. In this model, independent sources turn on randomly and instantaneously ionize a sphere with comoving radius  $R$ , which then remains ionized. The rate of source creation is such that the mean ionization fraction is zero prior to  $z_{\text{ion}} + \delta z$  and then rises linearly with redshift to unity at  $z_{\text{ion}}$ . GH derived the following approximate expression for the resulting power spectrum:

$$\begin{aligned} \frac{l^2 C_l}{2\pi} &= A l^2 \theta_0^2 e^{-l^2 \theta_0^2/2}, \\ \theta_0 &\equiv \frac{R}{\eta_0 - \eta_{\text{ion}}}, \\ A &= \frac{\sqrt{2\pi}}{36} \tau_0^2 \langle v^2 \rangle R / \eta_0 \delta z (1 + z_{\text{ion}})^{3/2} \end{aligned} \quad (18)$$

where  $\langle v^2 \rangle$  is the variance of peculiar velocities and  $\tau_0 \equiv \sigma_T \eta_0 n_0$  and  $n_0$  is the number density of free electrons today. The qualitative shape of this power spectrum is simple to understand. On large scales it is the shape of a white noise power spectrum ( $C_l = \text{constant}$ ), due to the lack of correlations between the patches. At small scales there is an exponential cutoff corresponding to the

angular extent of the patches themselves, since they have no internal structure.

The exact calculations for this model by KSD result in a very similar shape but with the power reduced by a factor of two and the location of the peak shifted to larger  $l$  by 30%. Thus we can write down very simple, and accurate, equations for the location of the maximum, which are those of GH with the prefactors modified to fit the results of KSD:

$$\begin{aligned} \left( \frac{l^2 C_l}{2\pi} \right)_{\text{max}} &= \frac{\sqrt{2\pi}}{36e} \tau_0^2 \langle v^2 \rangle R / \eta_0 \delta z (1 + z_{\text{ion}})^{3/2}, \text{ and} \\ l_{\text{max}} &= \frac{1.8\eta_0}{R} \left[ 1 - (1 + z_{\text{ion}})^{-1/2} \right]. \end{aligned} \quad (19)$$

Note that for sufficiently large  $R$ , velocities are not coherent within a patch and equations 18 and 19 break down; cancellations once again become important. However, this only happens for  $R \gtrsim 10$  Mpc since the velocity correlation function only becomes negative for separations greater than about  $30h^{-1}$  Mpc (KSD). As long as  $R$  is less than 10's of Mpc, the power scales linearly with  $R$ .

Aghanim et al. (1996, hereafter ‘‘A96’’) used a slightly more complicated model in which there was a distribution of patch sizes due to an assumed distribution of mini-quasar luminosities. The larger patches dominate at low  $l$  and the cutoff at higher  $l$  is much softer than in the single patch case, due to the existence of the smaller patches. For an order-of-magnitude calculation, their largest patches have  $R \simeq 10$  Mpc and reionization proceeds from  $z_{\text{ion}} + \delta z = 10.6$  to  $z_{\text{ion}} = 5.6$ . For this simplification of the A96 model we find the curve in figure 3 which has  $\left( \frac{l^2 C_l}{2\pi} \right)_{\text{max}} \simeq 1 \times 10^{-12}$  and  $l_{\text{max}} \simeq 1300$ .

This amplitude is just large enough to possibly be a source of systematic error in the determination of cosmological parameters from *MAP* data, which has sensitivity out to  $l \simeq 1000$ . To be more precise, *MAP* can determine the power in a broad band centered on  $l = 800$  with width  $\delta l = 400$  to about 0.5 %. Thus, given the primary signal assumed in the figure, we may expect signals on the order of  $5 \times 10^{-13}$  to be significant contaminants. This IHR signal from a 10 Mpc patch would be an even more noticeable effect in the *Planck* data since *Planck* has sensitivity out to about  $l \simeq 2000$  and can determine the power in a broad band centered on  $l = 1500$  with width  $\delta l = 1000$  to about 0.2 %.

The quasar luminosity function (QLF) is relatively well measured in the optical below redshift  $z < 5$ , with a typical average optical luminosity of  $10^{46}$  erg s $^{-1}$ . In order to estimate the expected typical HII patch size around the observed quasars, one needs to know their

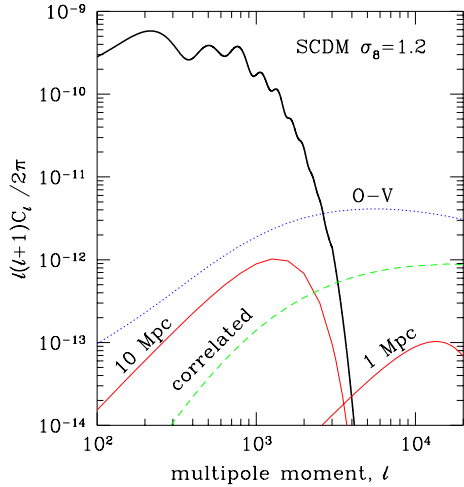


Fig. 3.— The thick solid line is the angular power spectrum of the primary CMB anisotropy in the standard cold dark matter (SCDM) model, normalized so that the fractional rms fluctuations of the mass in  $8h^{-1}$  Mpc spheres is  $\sigma_8 = 1.2$ . The other curves are contributions to the power spectrum expected from different models of IHR. The light solid curves are for the uncorrelated model (see equation 18) with  $z_{\text{ion}} = 5.6$  and  $\delta z = 5$  with comoving patch radii of  $R = 10$  Mpc and  $R = 1$  Mpc. The dashed curve is for the correlated model of KSD which achieves full reionization at  $z_{\text{ion}} = 26$ . The underlying model is spatially flat CDM with  $\Omega_b = 0.1$  and  $h = 0.5$ . The expected O-V effect for this same model with the same reionization redshift is also shown, calculated using the formalism of Jaffe & Kamionkowski (1998).

lifetime (or “duty-cycle”). Taking the lifetime of quasars to be universal, and near the Eddington time ( $\sim 5 \times 10^7$  yr), and further ignoring recombinations, one obtains a comoving radius of  $\sim 10$ – $20$  Mpc. As seen above, this would be large enough for its effects on the CMB to be detectable by *Planck* and maybe *MAP*.

We emphasize however, that the typical quasar luminosity at  $z = 10$  can be much lower than at  $z \sim 3$ . In hierarchical structure formation models, the nonlinear mass-scale is  $\sim 3$  orders of magnitude smaller at  $z = 10$  than at  $z \sim 3$ . With a linear scaling between quasar luminosity and halo mass, this would reduce the average patch-size by a factor of  $\sim 10$ . In addition, the duty-cycles of quasars are not well established. In theoretical models where the QLF is derived by associating quasars with collapsed dark halos (in the Press–Schechter formalism), a typical lifetime of  $\sim 5 \times 10^7$  yr would generically lead to an overestimate of the number of observed quasars (e.g. Small & Blandford 1992). To avoid these overpredictions, one needs to assume that either (1) the quasar shines at a small fraction of the Eddington luminosity, or (2) the efficiency of black hole formation, expressed as  $M_{\text{bh}}/M_{\text{halo}}$ , is 2 orders of magnitude lower than suggested by nearby galaxies (Magorrian et al. 1998), or (3) the black hole masses grow in an optically inactive phase (e.g. Haehnelt, Natarajan & Rees 1998). Alternatively, one can fit the observed QLF by assuming that the quasar lifetime is  $\sim 100$  times shorter than the Eddington time (Haiman & Loeb 1997). In the latter case, the HII patch sizes would be reduced to  $R \lesssim 1$  Mpc (i.e. reionization would correspond to a larger number of smaller patches).

According to equation 19, patches smaller than a few Mpc result in power spectra with smaller maxima at values of  $l$  that are too high, and well outside the range of sensitivity of *MAP* and *Planck*. Even for patches as large as 1 Mpc, one can see that, at least for reionization at the extreme low end of the redshift range, their effect is negligible (see figure 3). A detection of an IHR signal in the CMB with a peak could have important implications for quasar evolution theories, e.g. by ruling out models that lead to short duty cycles and small patch sizes. A detection might also prove that reionization was caused by mini-quasars, rather than mini-galaxies, since for the mini-galaxy models, the patch sizes are expected to be only a few hundred kpc. However, in light of the small expected patch sizes, it seems unlikely that *MAP* or *Planck* reaches the required angular resolution for such a detection.

The above calculations of the IHR power spectrum all assumed that the ionized regions are uncorrelated. However, the pattern of density fluctuations will affect the

pattern of ionized regions and therefore correlations in the density field should give rise to correlations in the ionization fraction field. Determining what these correlations should be is complicated by the fact that the density field affects the ionization field in two different ways: by the fact that the sources are most likely located in high density regions and the fact that the recombination rates are highest in the densest regions.

To take the former effect into account, KDS gave the ionization field the same correlation structure as that of the “high-peaks” of the density field. These high-peaks are regions where the fractional density perturbation,  $\delta = \frac{\delta\rho}{\rho}$ , smoothed on the appropriate scale, exceeds the critical value for spherical collapse. The smoothing scale was taken to be that corresponding to  $10^8 M_\odot [(1+z)/11]^{-3/2}$ , since objects below this size will not be able to cool sufficiently to fragment and form stars (Haiman, Rees & Loeb 1997). One further assumption was that the sources ionized a region  $E$  times larger than that from which they collapsed where the efficiency factor is time-dependent and given by (Haiman & Loeb 1997, Haiman & Loeb 1998a)  $E = 7 \times 10^5 (\eta/\eta_0)^6$ . For this rather high choice for the efficiency, reionization is complete at  $z_{\text{ion}} = 26$ .

The resulting spectrum is shown as the dashed line in figure 3. The correlations between the patches—which are individually only hundreds of kiloparsecs in radius—drastically alter the low  $l$  shape. Even given the high redshift of reionization in this scenario, the corresponding uncorrelated model of equation 18 would predict orders of magnitude less power at  $l \sim 10^3$  to  $10^4$ .

If this signal were in the data, but not in ones model of the data, it would lead to a bias in the determination of cosmological parameters. KSD estimated the bias that would occur in a nine parameter fit, assuming the primary signal was that of standard cold dark matter. For Planck, the systematic in the estimate of the baryon density was equal to the statistical error. For all the other parameters the systematic error was less than the statistical error.

### 3.4. Discussion

If the mini-quasar scenario is correct, with bright, long-lived quasars, then the Doppler effect will lead to a significant contamination of the *Planck* data and possibly a marginally important one for *MAP* data. For the more likely mini-galaxy scenario, if one ignores the correlations in the ionized patches, the contamination is completely irrelevant for both *MAP* and *Planck*. However, correlations may indeed be important, and in one attempt to take them into account, we have seen that

for an extreme mini-galaxy scenario, the contamination is marginally significant for *Planck*.

Work by Oh (1999) supports the idea that the ionized patches should be correlated. Oh has modeled the ionizing sources as characterized by a mean separation (given by Press-Schechter theory), an isotropic attenuation length which specifies how far the ionizing radiation propagates, and a power-law correlation function (appropriate for these highly-biased objects). Placing sources in a box and working out the resulting flux densities he can then calculate the correlation function of the flux density. It is indeed correlated, with significant (0.2) correlation at a comoving separations of 10 Mpc. Although a clumping factor for the IGM from Gnedin & Ostriker (1997) is used to estimate the attenuation length, all propagation from the sources is taken to be isotropic, and hence this work does not yet include the influence of shielding and shadowing.

As one can see in Fig. 3, the contribution from IHR may be sub-dominant to that from the Ostriker-Vishniac (O-V) effect, as it is for all three models of IHR shown. The O-V contribution here is calculated using the formalism of Jaffe & Kamionkowski (1998, hereafter “JK98”). One must keep in mind that as a second-order effect, it is highly sensitive to the normalization. The curve here is COBE-normalized ( $\sigma_8 = 1.2$ ); a cluster normalization of  $\sigma_8 = 0.6$  would reduce the  $C_l$  by a factor of 16. It is also calculated for the very early reionization redshift (and resulting high optical depth) of  $z_{\text{ion}} = 26$ . However, the amplitude is not very sensitive to  $\tau$  because much of the effect actually comes from more recent times—the dropping number density of electrons must compete with the growth in the density contrasts and peculiar velocities (Hu & White 1995, JK98). Of course, the separation into IHR and O-V is artificial, and efforts to understand the contribution from reionization are surely going to benefit from treating them simultaneously. Indeed, the 2-point function of  $\hat{\tau}\hat{\gamma} \cdot \mathbf{v}_e$ , measured from a simulation, would include both effects.

Gravity is the only other late-time, frequency-independent, influence on the CMB photons, causing lensing and the Rees-Sciama effect (Rees & Sciama 1968). The angular-power spectrum from the Rees-Sciama effect has been calculated by Seljak (1995) and is substantially sub-dominant to either the primary spectrum or the O-V effect at all angular scales. Gravitational lensing results in a smearing of the primary CMB angular power spectrum and has also been calculated by Seljak (1996). Uncertainties in this calculation may indeed be important for any attempt to recover the contribution from the IHR and Ostriker-Vishniac effects.

#### 4. Conclusions

The principal unanswered questions about reionization are: what type of sources caused it, and at what redshift did it occur? These questions have been addressed both theoretically and observationally. From a theoretical point of view, the two leading candidate sources are an early generation of stars (“mini-galaxies”), or massive black holes in small halos (“mini-quasars”). It is possible to estimate the efficiencies with which objects form in the earliest collapsed halos: from the metals in the Ly $\alpha$  forest, and from the evolution of the quasar luminosity function at  $z < 5$ , respectively. However, the uncertainties in these efficiencies are still too large to allow definite predictions. The expected reionization redshift, depending on the type of source, cosmology, power spectrum, and a combination of the efficiency factors, is between  $7 \lesssim z \lesssim 20$  in homogeneous models. A further complication is the inhomogeneous nature of reionization: the sources of ionizing radiation are likely clustered, and embedded in complex dense regions, such as the filaments and sheets seen in 3D simulations. At the same time, the gas to be ionized likely has significant density fluctuations.

Further theoretical progress on the problem will likely come from 3D simulations. Such simulations must be able to follow the propagation of a non-spherical ionization front into a medium that has large density fluctuations, as well as opaque clumps of absorbing material. In a homogeneous medium populated by randomly distributed sources, the background radiation would have negligible fluctuations (e.g. Zuo 1992). However, because the density inhomogeneities absorb the UV flux of the ionizing sources, and re-emit diffuse ionizing photons as they recombine, the ionizing background will likely become significantly inhomogeneous and anisotropic (Norman et al. 1998). The first numerical algorithms to deal in full detail with these problems have been proposed by Abel, Norman & Madau (1998) and Razoumov & Scott (1998) (see also Gnedin 1998).

The reionization redshift can also be constrained observationally, with a resulting uncertainty that is comparable to the theoretical range:  $6 \lesssim z \lesssim 40$ . On both ends of this redshift range, observational progress is likely in the near future. If new Ly $\alpha$  emitters are discovered at higher redshifts, this would improve the lower bound. Conversely, as the CMB data are collected, the constraint on the electron scattering optical depth will improve, tightening the upper bound.

We have seen how the optical depth to Thomson-scattering, and hence the epoch of reionization, can be constrained by determining the amount of damping in the

CMB temperature anisotropy and by detection of the polarization contribution at very large angular scales. The spatial inhomogeneity of the reionization process gives us a further opportunity to probe in more detail the epoch of reionization. For this probe to become reality, further development of theoretical predictions is required, as well as more sensitive measurements at arc minute and smaller angular scales.

Fortunately, the inhomogeneity of reionization is unlikely to spoil our ability to interpret the primary CMB anisotropy, to be measured with exquisite precision over the next decade, although this may not be the case if reionization did indeed occur via mini-quasars. For the mini-galaxy models, even when reionization occurs at the very high end of the allowed redshift range, very little signal is produced at the relevant angular scales. Further progress in these predictions is likely to be motivated by the desire to understand the spectrum at  $l \gtrsim 3000$  as a means of probing the end of the dark ages, rather than at  $l \lesssim 3000$ , as a possible contaminant of the primary signal.

We are grateful to our collaborators S. Dodelson, A. Loeb, M. Rees, and R. Scoccimarro for contributing to our understanding of this subject, to A. Jaffe for supplying the “O-V” effect curve in Fig. 3, and to M. Norman for supplying Fig. 2. ZH was supported at Fermilab by the DOE and the NASA grant NAG 5-7092.

#### References

- Abel, T., Norman, M. L., & Madau, P. 1998, ApJL, submitted, preprint astro-ph/9812151
- Aghanim, N., Désert, F. X., Puget, J. L., & Gispert, R. 1996, A&A, 311, 1
- Arons, J., & Wingert, D. W. 1972, ApJ, 177, 1
- Baltz, E. A., Gnedin, N. Y., & Silk, J. 1998, ApJL, 493, 1
- Barkana, R., & Loeb, A. 1999, ApJ, submitted, preprint astro-ph/9901114
- Baugh, C. M., Cole, S., Frenk, C. S. & Lacey, C. G. 1998, ApJ, 498, 504
- Bouchet, F. R., Prunet, S., Sethi, K. S., preprint astro-ph/9809353
- Carr, B. J., Bond, J. R. & Arnett, W. D. 1986, ApJ., 306, L51
- Conti, A., Kennefick, J. D., Martini, P., & Osmer, P. S. 1999, AJ, in press, astro-ph/9808020
- Couchman, H. M. P. & Rees, M. J. 1986, MNRAS, 221, 53
- Dodelson, S. & Jubas, J. 1995, ApJ, 439, 503
- Elvis, M., Wilkes, B. J., McDowell, J. C., Green, R. F.,

- Bechtold, J., Willner, S. P., Oey, M. S., Polomski, E., & Cutri, R. 1994, *ApJS*, 95, 1
- Eisenstein, D. J., Hu, W., Tegmark, M., preprint astro-ph/9807130
- Fabian, A. C. & Barcons, X. 1992, *ARA&A*, 30, 429
- Fardal, M. A., Giroux, M. L., & Shull, J. M. 1998, *AJ*, 115, 2206
- Fixsen, D. J., Cheng, E. S., Gales, J. M., Mather, J. C., Shafer, R. A., & Wright, E. L. 1996, *ApJ*, 473, 576
- Fixsen, D. J., Dwek, E., Mather, J. C., Bennett, C. L., Shafer, R. A., 1998, *ApJ*, inpress, preprint astro-ph/9803021.
- Fukugita, M. & Kawasaki, M. 1994, *MNRAS*, 269, 563.
- Gibilisco, M. 1996, *Int. J. Mod. Phys. A*11, 5541, preprint astro-ph/9611227
- Gnedin, N. Y. 1998, in *Proc. of 19<sup>th</sup> Texas Symposium on Relativistic Astrophysics and Cosmology*, held in Paris, France, Dec. 14-18, 1998, Eds. J. Paul, T. Montmerle, and E. Aubourg (CEA Saclay), in press
- Gnedin, N. Y., & Ostriker, J. P. 1997, *ApJ*, 486, 581
- Griffiths, L. M., Barbosa, D., Liddle, A. R. 1998, *MNRAS*, submitted, preprint astro-ph/9812125
- Gruzinov, A., & Hu, W. 1998, *ApJ*, in press, preprint astro-ph/9803188
- Gunn, J. E., & Peterson, B. A., 1965, *ApJ*, 142, 1633
- Haehnelt, M. G., Natarajan, P., & Rees, M. J. 1998, *MNRAS*, 300, 817
- Haiman, Z., Abel, T., & Rees, M. J. 1999, *ApJ*, to be submitted
- Haiman, Z., & Loeb, A. 1997, *ApJ*, 483, 21
- Haiman, Z., & Loeb, A. 1998a, *ApJ*, 503, 505
- Haiman, Z., & Loeb, A. 1998b, *ApJ*, in press, preprint astro-ph/9807070
- Haiman, Z., & Loeb, A. 1998c, invited contribution to the Proceedings of 9<sup>th</sup> Annual October Astrophysics Conference, *After the Dark Ages: When Galaxies Were Young*, October 1998, College Park, MD, preprint astro-ph/9811395
- Haiman, Z., Madau, P., & Loeb, A. 1999, *ApJ*, in press, preprint astro-ph/9805258
- Haiman, Z., & Spaans, M. 1998, *ApJ*, in press, preprint astro-ph/9809223
- Haiman, Z., Rees, M. J., & Loeb, A. 1997, *ApJ*, 476, 458
- Hauser, M. G. 1998, *ApJ*, 508, 25
- Hu, E. M., Cowie, L. L., & McMahon, R. G. 1998, *ApJ*, 502, 99
- Hu, W., & White, M. 1995, *Astronomy and Astrophysics* 315, 33
- Hu, W., & White, M. 1997, *ApJ*, 479, 568
- Hu, W., Scott, D. & Silk, J. 1994, *Phys. Rev. D*49, 648
- Jaffe, A. H., & Kamionkowski, M., *Phys. Rev. D*58, 1998, 043001
- Kaiser, N. 1984, *ApJ*, 282, 374
- Knox, L., Scoccimarro, R., Dodelson, S., 1998, *Phys. Rev. Lett.*, 81, 2004
- Knox, L., 1998, preprint astro-ph/9811358
- Loeb, A., & Haiman, Z. 1997, *ApJ*, 490, 571
- Ma, C.-P. & Bertschinger, E. (1995), *ApJ*, 455, 7
- Madau, P., Haardt, F., & Rees, M. J. 1998, *ApJ*, submitted, preprint astro-ph/9809058
- Madau, P., Meiksein, A., & Rees, M. J. 1997, *ApJ*, 475, 429
- Magorrian, J., et al. 1998, *AJ*, 115, 2285
- Meiksin, A., & Madau, P. 1993, *ApJ*, 412, 34
- Miralda-Escudé, J. 1998, *ApJ*, 501, 15
- Miralda-Escudé, J., Haehnelt, M., & Rees, M. J. 1999, *ApJ*, submitted, preprint astro-ph/9812306
- Miralda-Escudé, J., & Rees, M. J. 1994, *MNRAS*, 266, 343
- Nath, B. B., & Bierman, P. L. 1993, *MNRAS*, 265, 241
- Norman, M. L., Paschos, P., & Abel, T. 1998, in *Proc. of H<sub>2</sub> in the Early Universe*, Workshop held in Florence, Italy, eds. E. Corbelli, D. Galli, and F. Palla, *Memorie Della Societa Astronomica Italiana*, p. 455
- Oh, S.P., work in progress
- Ostriker, J. P., & Vishniac, E. T., 1986, *ApJL*, 306, 51
- Ostriker, J. P., & Gnedin, N. Y. 1996, *ApJ*, 472, 603
- Ostriker, J. P., & Cowie, L. L., 1981, *ApJL*, 243, 127
- Pei, Y. C. 1995, *ApJ*, 438, 623
- Prunet, S., Sethi, K. S., Bouchet, F. R., preprint astro-ph/9803160
- Press, W. H., & Schechter, P. L. 1974, *ApJ*, 181, 425
- Puget, J.-L., Abergel, A., Bernard, J.-P., Boulanger, F., Burton, W. B., Desert, F.-X., Hartmann, D., 1996, *A&A* 308, L5
- Rauch, M., Miralda-Escudé, J., Sargent, W. L. W., Barlow, T. A., Weinberg, D. H., Hernquist, L., Katz, N., Cen, R., & Ostriker, J. P. 1997, *ApJ*, 489, 7
- Razoumov, A., & Scott, D. 1998, *MNRAS*, submitted, preprint astro-ph/9810425
- Rees, M. J., & Sciama, D. W. 1968, *Nature*, 517, 611
- Reimers, D., Köhler, S., Wisotzki, L., Groote, D., Rodriguez-Pascual, P., & Wamsteker, W. 1997, *A&A*, 326, 489
- Reisenegger, A., & Miralda-Escudé, J. 1995, *ApJ*, 449, 476

- Scalo, J. M. 1986, *Fundamentals of Cosmic Physics*, vol. 11, p. 1-278
- Sciama, D. W. 1993, *Modern Cosmology and the Dark Matter Problem*, Cambridge University Press
- Scott, D., & Rees, M. J. 1990, MNRAS, 247, 510
- Seljak, U. 1995, preprint astro-ph/9506048
- Seljak, U., 1996, ApJ, 463, 1
- Schlegel, D. J., Finkbeiner, D. P., Davis, M., 1998, ApJ, 500, 525
- Shapiro, P. R., Raga, A. C., & Mellema, G. 1997, in *Structure and Evolution of the IGM from QSO Absorption Line Systems*, 13<sup>th</sup> IAP Colloquium, eds. P. Petitjean and S. Charlot (Paris: Editions Frontiere), in press, preprint astro-ph/9710210
- Shapiro, P. R., & Giroux, M. L. 1987, ApJ, 321, L107
- Shapiro, P. R., Giroux, M. L., & Babul, A. 1994, ApJ, 427, 25
- Shapiro, P. R., Giroux, M. L., & Kang, H. 1987, in *High Redshift and Primeval Galaxies*, eds. J. Bergeron, D. Kunth, B. Rocca-Volmerange, and J. Tran Thanh Van (Paris: Editions Frontieres), pp. 501-515
- Shaver, P., Windhorst, R. A., Madau, P., & de Bruyn, A. G. 1999, A&A, submitted, preprint astro-ph/9901320
- Small, T. A., & Blandford, R. D. 1992, MNRAS, 259, 725
- Songaila, A., & Cowie, L. L. 1996, AJ, 112, 335
- Stebbins, A., & Silk, J. 1986, ApJ, 300, 1
- Sunyaev, R. A. 1978, in *Large-Scale Structure of the Universe*, eds. M.S. Longair & J. Einasto (Dordrecht: Reidel), p. 393
- Tegmark, M., Silk, J., & Blanchard, A. 1994, ApJ, 420, 484
- Thompson, R., et al. 1998, preprint astro-ph/9810285
- Tytler, D. et al. 1995, in *QSO Absorption Lines*, ESO Astrophysics Symposia, ed. G. Meylan, Springer, Heidelberg, p.289
- Vishniac, E. T., ApJ, 1987, 322, 597.
- Wadsley, J. W., Hogan, C. J., Anderson, S. F. 1998, to appear in the proceedings of "After the Dark Ages: When Galaxies were Young (the Universe at  $2 < z < 5$ )", 9th Annual October Astrophysics Conference in Maryland, preprint astro-ph/9812239
- Weinberg, D. H., Miralda-Escudé, J., Hernquist, L., & Katz, N. 1997, ApJ, 490, 564
- Weymann, R.J., Stern, D., Bunker, A., Spinrad, H., Chaffee, F.H., Thompson, R.I., & Storrie-Lombardi, L.J. 1998, ApJL, 505, 95
- Zaldarriaga, M., Spergel, D., & Seljak, U. 1997, ApJ, 488, 1
- Zhang, Y., Meiksin, A., Anninos, P., & Norman, M. L. 1998, ApJ, 495, 63
- Zuo, L. 1992, MNRAS, 258, 36